Roughness characterization of porous soil with acoustic backscatter

Michael L. Oelze,[a] James M. Sabatier, and Richard Raspet
National Center for Physical Acoustics and Department of Physics and Astronomy, University of Mississippi, University, Mississippi 38677

(Received 28 November 2000; revised 22 February 2001; accepted 23 February 2001)

The use of acoustics to determine the pore properties of soils, such as porosity, permeability, and tortuosity, is well established. A theoretical surface impedance and complex bulk wavenumber was developed by K. Attenborough for porous media that incorporated the soil pore properties as parameters [J. Acoust. Soc. Am. **73**, 785–799 (1983)]. Acoustic level difference measurements were used as a noninvasive means of finding the soil pore properties. Acoustic reflection measurements showed that the sound field over porous rough surfaces is modified by the surface impedance and by surface roughness. It is not possible to separate the signal modification due to impedance and the signal modification from roughness scattering in a forward scattering measurement. In order to accurately determine the soil pore properties, the roughness effects must be known independently from the surface impedance. A means of measuring roughness apart from impedance would allow the effects of roughness to be taken out of the level difference measurements. The underwater acoustics community has used acoustic backscatter for many years to examine surface roughness. The feasibility of adapting these acoustic backscatter techniques to outdoor porous soil surfaces is examined.
[DOI: 10.1121/1.1366320]

PACS numbers: 43.20.Fn, 43.30.Hw [ANN]

I. INTRODUCTION

Predictions of sound propagation over porous soil using three pore parameters have been fit to measured data to determine the pore properties. This work was based upon models constructed by Attenborough to characterize the properties of porous media.[1] The Attenborough models have been extensively compared to soil measurements and therefore are useful for modeling the range expected.[2,3] These models calculate the complex bulk density and bulk wavenumber from the porosity, tortuosity, and flow resistivity of soils. The low frequency limits of the density and wavenumber are given by

$$\rho_b(\omega)=\frac{\rho_0}{\Omega}\left(\frac{4}{3}T+i\frac{4\sigma_{\mathrm{eff}}}{\omega\rho_0}\right), \tag{1}$$

$$k_b(\omega)=k_0\sqrt{\gamma}\left(aT+i\frac{4\sigma_{\mathrm{eff}}}{\rho_0\omega}\right)^{1/2}. \tag{2}$$

In these equations γ is the ratio of specific heats in air, k_0 is the wavenumber in air, ρ_0 is the density of air, T is the tortuosity, Ω is the porosity, $\sigma_{\mathrm{eff}}=s_p^2\sigma\Omega$ is the effective flow resistivity with s_p^2 the pore shape factor and σ the flow resistivity, and a is defined by

$$a=\frac{4}{3}-\left(\frac{\gamma-1}{\gamma}\right)N_{\mathrm{Pr}},$$

where N_{Pr} is the Prandtl number. The bulk density and bulk wavenumber of the soil can be combined to calculate the normalized surface impedance

$$Z(\omega)=\left[\frac{1}{\rho_0 c_0}\right]\left[\frac{\omega\rho_b(\omega)}{k_b(\omega)}\right], \tag{3}$$

where c_0 is the speed of sound in air.

In a review of sound propagation over a smooth impedance surface, calculations of the sound pressure level emanating from a point source are described by Attenborough *et al.*[4] In that review paper, the sound pressure level is determined by the source-receiver geometry, the frequency of interest, and the impedance of the surface. The received sound level is the combination of the direct signal from the source to receiver and the signal reflected off of the surface. The reflected signal contains information about the surface since it is altered in amplitude and phase upon reflection. This information is embedded in a reflection coefficient, which is a function of the angle of incidence and the surface impedance. Information about the porous properties of the soil can be inferred from the value and frequency dependency of the surface impedance. Sabatier *et al.* used the acoustic level difference technique illustrated in Fig. 1 to measure the pore properties of soils.[2] The level difference technique is attractive because it is noninvasive method of measuring pore properties. Later work showed only the ratio of tortuosity/porosity and flow resistivity/porosity could be determined.[3]

In taking the level difference measurements, it was found that the experimental results matched fairly well with the developed models over smooth surfaces. However, when the theoretical model was compared with results from ex-

[a]Present address: Bioacoustics Research Laboratory, Department of Electrical and Computer Engineering, University of Illinois at Urbana–Champaign, 405 North Mathews Avenue, Urbana, IL 61801. Electronic mail: oelze@brl.uiuc.edu

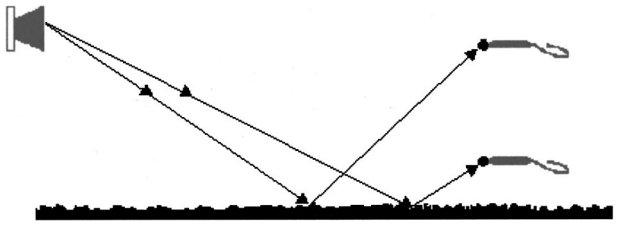

FIG. 1. Level difference measurement experimental setup showing sound source and two vertically separated microphones above the ground surface.

periments over rough surfaces, the agreement diverged. Hence, roughness was causing a significant effect upon the forward propagation of sound.

Attenborough proposed that the roughness of a surface might be able to be characterized by examining the sound reflected from the surface.[5] Efforts were then made to model the effects of roughness on the propagation of sound over porous surfaces. Attenborough *et al.* chose to treat roughness as an effective admittance, or inverse impedance.[6]

Attenborough used the analysis by Howe[7] for constructing an effective admittance for hemispherical roughness elements, valid for low grazing angles. In this model, the rough surface was treated as a smooth surface with an altered admittance. Combining Howe's results with results from Tolstoy,[8] Attenborough derived an effective admittance for roughness scatterers of arbitrary shape. The effective admittance is

$$\beta_3^* = \beta_s - i(k_0\sigma_v/2 + \beta_s k_b \sigma_v), \tag{4}$$

where β_s is normal surface admittance, $1/Z$, and σ_v is the roughness length scale defined as the projected volume of roughness per unit area of the surface. In laboratory experiments, the model predicted the effects of roughness well.[5]

Using the effective admittance from Attenborough, roughness experiments were conducted by Chambers on porous surfaces.[9] The experimental setup by Chambers was similar to Attenborough's level difference method except that the source and receiver were placed closer to the ground. In so doing, the patch ensonified by the source had a larger footprint. It was postulated that by allowing a larger area to react with the sound field, a better representation of the surface roughness could be obtained since local anomalies of rough or smooth sections would be averaged.

Chambers observed that the effects of roughness mimicked those of porosity and permeability. Roughness acts to decrease reflected sound levels for the grazing incidence geometry due to scattering. Increasing the permeability or porosity of a surface also decreases sound levels due to changes in viscous drag forces within the pore spaces of the ground. In the models themselves, the roughness and the other soil properties are not independent and, therefore, experimentally it is impossible to measure the effects independently. If one does not properly characterize the soil properties for the porosity and permeability with some other method, the observed acoustic response may be inaccurately apportioned between the effects of roughness and the other soil properties. The result is that measurements of the roughness scale will be inaccurate. The models may accurately describe the effects of roughness if the relevant assumptions are not violated and the soil properties are properly characterized. It may also be that the models for forward scattering need to be altered to better describe the field test data.

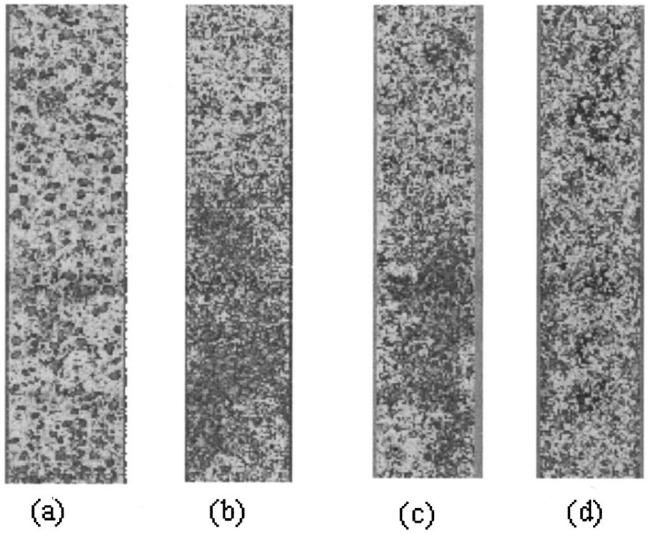

FIG. 2. Height profiles of four soil plots taken by laser microreliefmeter.

II. ROUGHNESS STATISTICS OF OUTDOOR SOIL SURFACES

One method that has been used to measure surface roughness without the effects of the acoustic surface impedance is the laser microprofiler.[10] The laser microprofiler measures the height profile of a surface with a resolution of 0.25 mm in the vertical direction and in square sections of $0.5 \times 0.5\,\mathrm{mm}^2$ in the horizontal. Römkens *et al.* used the laser profiler to measure the roughness of several soil surfaces.[11] Figure 2 shows profiles of four different soil tracts measured by the laser profiler.

From a surface profile, the roughness power spectrum can be derived. The power spectrum is the squared magnitude of the Fourier transform of the surface profile. The rms height and the correlation function can be derived from the 2-D power spectrum $W(k)$ by integrating over the roughness wavenumber, k, giving

$$h_{\mathrm{rms}}^2 = 2\pi \int_{k_c}^{\infty} W(k) k\, dk, \tag{5}$$

$$C(x) = \frac{2\pi}{h_{\mathrm{rms}}^2} \int_{k_c}^{\infty} W(k) e^{-ikx} k\, dk, \tag{6}$$

where k_c is the cutoff wavenumber. The correlation length is the length at which $C(x)$ decreases to $1/e$ of its initial value and describes how the roughness elements are packed together on the surface. The larger the correlation length for the roughness the more sparse the roughness elements are spread about on the surface.

Intuitively, not all scales of roughness will be included in any surface profile since the profile will have a finite length. The low wavenumber cutoff is chosen appropriate to the size of the roughness being examined. For example, if a low wavenumber cutoff were chosen which corresponds to a

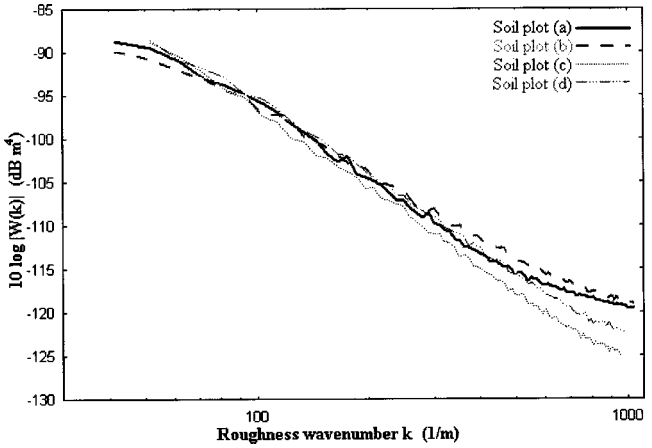

FIG. 3. Two-dimensional Power spectrums for the four soil profiles of Fig. 2 plotted in log–log space.

cutoff wavelength of several kilometers, the roughness of local hills and valleys would be incorporated into the statistics evaluated from the power spectrum. The cutoff wavelength determines the size of the plot from which the statistics of the surface are calculated. Appropriate cutoff wavenumbers for normal agricultural soil surfaces would correspond to wavelengths of a meter or less. Any values of rms height and correlation length should be given with reference to the cutoff wavenumber chosen.

Figure 3 shows the 2-D power spectrums for the four profiles of Fig. 2 obtained by the laser profiler. The soil plots were made by breaking up the soil into clods using various farming implements. As the soil is worked the larger clods continue to be broken down into smaller and smaller clods. Kolmogorov predicted that a process where particles are broken down into smaller and smaller particles would have a power law distribution.[12] The 2-D power spectrums in Fig. 3, which were plotted in log–log space, show that the power spectra for the soil profiles are also power laws over a range of wavenumbers. The power laws of the power spectrum for the random rough surfaces are of dimensionality such that the surfaces are fractal, which means the surfaces contain structure on all scales and the form of the structure is similar at each scale.

III. UNDERWATER BACKSCATTER

The underwater community has utilized acoustic backscatter techniques for many years to examine the roughness of ocean surfaces. For a review of acoustic backscatter in underwater sound, see Ref. 13. Backscatter is measured in terms of the scatter strength, which is defined as

$$S_s = 10 \log \sigma_s(\theta), \tag{7}$$

where σ_s is the backscatter cross-section.[14] The backscatter cross-section is determined by looking at the ratios of the scattered intensity to the intensity incident upon the surface. The cross-section is given by

$$\sigma(\theta) = \frac{r^2}{A}\frac{I_s}{I_0}, \tag{8}$$

where θ is the grazing angle, r is the distance from source to surface, A is the area of the ensonified surface, and I_s and I_0 are the scattered and incident intensities.

Scattering from rough surfaces can be modeled by use of small roughness perturbation theories. For rough surfaces, perturbation theory is valid under the restriction[13]

$$k_a h < 0.5, \tag{9}$$

where h is the rms height of the surface. First order perturbation theory under Dirichlet boundary conditions yields for the backscatter cross-section[15]

$$\sigma_p(\theta) = 4k_a^4 \sin^4 \theta\, W(2k_a \cos\theta), \tag{10}$$

where k_a is the acoustic wavenumber and $W(2k_a \cos\theta)$ is the 2-D power spectrum evaluated at the roughness wavenumber, $2k_a \cos\theta$. While scattering occurs at many points within the ensonified surface, only scatter points with roughness wavenumber separation on the surface equal to $2k_a \cos\theta$ are in phase for a given graze angle and wavelength of sound. Hence, the scatter contribution will predominately come from the wavenumber, $2k_a \cos\theta$, which is the Bragg wavelength.[16] In principle, the roughness power spectrum can be evaluated by inverting scatter strength measurements taken at different frequencies and graze angles. This would give the power spectrum in terms of a logarithmic function

$$10 \log W(k,\theta) = S_s(k,\theta) - 10 \log 4k^4 \sin^4 \theta. \tag{11}$$

It has been shown that profiles of underwater surfaces tend to have power roughness spectrums with power law behaviors similar to those for soil surfaces.[17,18] The fact that the power spectrums are power law means that in log-log space the power spectrum is linear. Theoretically this means that all that is needed to approximate the full power spectrum is two data points from which the slope and intercept of the spectrum line can then be calculated. The power law characteristic of the roughness power spectrum has been utilized to examine statistics of underwater surfaces.[18]

IV. BACKSCATTER FROM POROUS SOIL SURFACES

The success of underwater acoustic backscatter at examining sea floor roughness and the fact that agricultural soil surfaces display the power law behavior indicates that backscatter may be a viable means of measuring roughness of porous soil surfaces. The value of using acoustic backscatter on porous soil surfaces depends upon the ability of backscatter to give roughness statistics independent of the surface impedance effects. The effect of surface impedance on backscatter is investigated by incorporating impedance boundary conditions into the calculation of the perturbation cross-section.

Figure 4 shows the boundary of a rough surface of finite impedance with the incident, reflected, and transmitted velocity potentials given by

$$\Phi i = e^{-ik_1[\beta_{1x}x + \beta_{1y}y + \beta_{1z}z]}, \tag{12a}$$

$$\Phi r = \int\int e^{-ik_1[\beta_{rx}x + \beta_{ry}y + \beta_{rz}z]} T_r(\mathbf{k}_r, \mathbf{k}_i)\, d\mathbf{k}_r, \tag{12b}$$

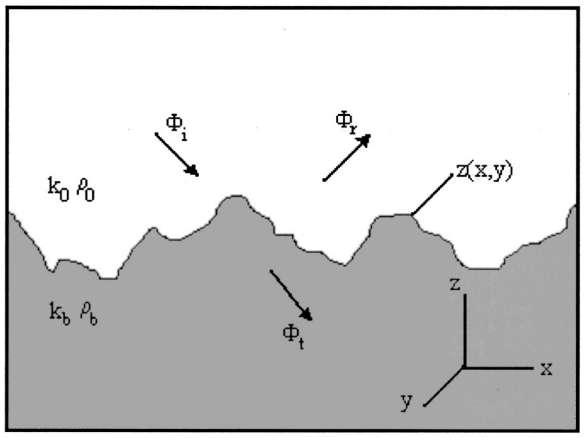

FIG. 4. Surface geometries for sound fields on a porous surface with roughness small compared to the wavelength.

$$\Phi t = \int\int e^{-ik_2[\beta_{tx}x+\beta_{ty}y+\beta_{tz}z]} T_t(\mathbf{k}_t,\mathbf{k}_i)\,d\mathbf{k}_t \tag{12c}$$

with the cosine angles represented by the β_{ij}'s, the $\mathbf{k}$'s representing the transverse acoustic wavenumbers, and T the transition matrix. The rms height of the roughness is assumed to be small compared to the wavelength of sound and the local slope is assumed to be small. To obtain the perturbation cross-section, the T-matrix is expanded in a power series in terms of h and S, the rms height and local slope of the surface, with

$$T_r = \sum_{m,n} h^m S^n T_{m,n}. \tag{13}$$

For a surface with height profile given by the function $z(x,y)$, the following relations hold:

$$\begin{aligned} &\langle z^2(x,y)\rangle = h^2, \quad z(x,y) = h\zeta(x,y), \\ &\langle \zeta^2(x,y)\rangle = 1, \quad S\zeta_i = \partial z/\partial x_i. \end{aligned} \tag{14}$$

The first-order correction to the T-matrix enables the first-order perturbation cross section to be calculated through the relation[19]

$$\sigma = (k_1\beta_{1z})^2 C(\mathbf{k}_r,\mathbf{k}_i), \tag{15}$$

$$\begin{aligned} C(\mathbf{k}_r,\mathbf{k}_i)\,\delta(\mathbf{k}_i-\mathbf{k}_i') = \langle (T_r(\mathbf{k}_r,\mathbf{k}_i) - \langle T_r(\mathbf{k}_r,\mathbf{k}_i)\rangle) \\ \times (T_r(\mathbf{k}_r,\mathbf{k}_i') - \langle T_r(\mathbf{k}_r,\mathbf{k}_i)\rangle)^*\rangle. \end{aligned} \tag{16}$$

To incorporate the soil surface pore properties, the boundary conditions for the continuous pressure and normal component of velocity at the surface are used:

$$\rho_1 \frac{\partial(\Phi_i+\Phi_r)}{\partial t} = \rho_2 \frac{\partial \Phi_t}{\partial t}, \tag{17}$$

$$\frac{\partial(\Phi_i+\Phi_r)}{\partial n} = \frac{\partial \Phi_t}{\partial n}. \tag{18}$$

Using the relation

$$\frac{\partial}{\partial n} = \frac{\partial}{\partial z} - S\left(\varsigma_i \frac{\partial}{\partial x_i}\right)_T \tag{19}$$

and solving the boundary condition equations for Φ_r in terms of Φ_i yields

$$\begin{aligned} &[-\rho\beta_{1z} + \kappa\beta_{tz} + S[\varsigma_j\beta_{1j}](\rho-1)]e^{-ik_1(\beta_{1j}x_j+\beta_{1z}z)} \\ &\quad = \int\int [-\rho\beta_{rz} - \kappa\beta_{tz} + S[\varsigma_j\beta_{rj}](1-\rho)] \\ &\qquad \times e^{-ik_1(\beta_{rj}x_j+\beta_{rz}z)} T_r\,d\mathbf{k}_r \end{aligned} \tag{20}$$

with

$$\rho = \frac{\rho_2}{\rho_1}, \quad \kappa = \frac{k_2}{k_1}.$$

Expanding the exponential

$$e^{-ik_1\beta_z z} = e^{-ik_1\beta_z h\varsigma(x,y)} \approx 1 - ik_1\beta_z h\varsigma(x,y)$$

and relating terms of order h^0S^0, h^1S^0, and h^0S^1 in Eq. (20) gives for h^0S^0

$$\begin{aligned} &(\rho\beta_{1z} - \kappa\beta_{tz})e^{-ik_1(\beta_{1j}x_j)} \\ &\quad = \int\int (\rho\beta_{rz} + \kappa\beta_{tz})e^{-ik_1(\beta_{rj}x_j)} T_{0,0}\,d\mathbf{k}_r; \end{aligned} \tag{21}$$

for h^1S^0

$$\begin{aligned} &(\rho\beta_{1z} - \kappa\beta_{tz})e^{-ik_1(\beta_{1j}x_j)}[-ik_1\beta_{1z}\varsigma(\mathbf{x})] \\ &\quad = \int\int (\rho\beta_{rz} + \kappa\beta_{tz})[(ik_1\beta_{1z}\varsigma(\mathbf{x}))T_{0,0} + T_{1,0}] \\ &\qquad \times e^{-ik_1(\beta_{rj}x_j)}\,d\mathbf{k}_r; \end{aligned} \tag{22}$$

for h^0S^1

$$\begin{aligned} &[\varsigma_j\beta_{1j}](\rho-1)e^{-ik_1(\beta_{1j}x_j)} \\ &\quad = \int\int \{[\varsigma_j\beta_{rj}](1-\rho)T_{0,0} \\ &\qquad - [\rho\beta_{rz} + \kappa\beta_{tz}]T_{0,1}\}e^{-ik_1(\beta_{rj}x_j)}\,d\mathbf{k}_r. \end{aligned} \tag{23}$$

The Fourier transform of Eq. (21) yields $T_{0,0}$; once $T_{0,0}$ is known, $T_{1,0}$ and $T_{0,1}$ can be obtained from the Fourier transforms of Eqs. (22) and (23). The results are

$$T_{0,0}(\mathbf{k}_r,\mathbf{k}_i) = \mathrm{R}\,\delta(\beta_{1x}-\beta_{rx})\,\delta(\beta_{1y}-\beta_{ry}), \tag{24}$$

$$T_{1,0}(\mathbf{k}_r,\mathbf{k}_i) = \frac{-1}{(2\pi)^2}\int\int_x 2ik_1\beta_{1z}\mathrm{R}e^{i(\mathbf{k}_r-\mathbf{k}_i)\cdot\mathbf{x}}\varsigma(\mathbf{x})\,d\mathbf{x}, \tag{25}$$

$$\begin{aligned} T_{0,1}(\mathbf{k}_r,\mathbf{k}_i) = \frac{1}{(2\pi)^2}\int\int_x \frac{(1-\rho)(1+\mathrm{R})}{\rho\beta_{rz}+\kappa\beta_{tz}} \\ \times(\varsigma_j\beta_{1j})e^{i(\mathbf{k}_r-\mathbf{k}_i)\cdot\mathbf{x}}\,d\mathbf{x}, \end{aligned} \tag{26}$$

where R is the Rayleigh reflection coefficient

$$\mathrm{R} = \frac{\rho\beta_{1z} - \kappa\beta_{tz}}{\rho\beta_{1z} + \kappa\beta_{tz}}. \tag{27}$$

The first order T's are seen to be related to the Fourier transform of the surface function by

$$hT_{1,0}(\mathbf{k}_r,\mathbf{k}_i) = -2ik_1\beta_{1z}\mathrm{R} \times\left\{\frac{1}{(2\pi)^2}\int\int_x z(\mathbf{x})e^{i(\mathbf{k}_r-\mathbf{k}_i)\cdot\mathbf{x}}d\mathbf{x}\right\}$$
$$hT_{1,0}(\mathbf{k}_r,\mathbf{k}_i) = -2ik_1\beta_{1z}\mathrm{R}Z(\mathbf{k}_r-\mathbf{k}_i), \tag{28}$$

where $Z(\mathbf{k}_r-\mathbf{k}_i)$ is the Fourier transform of the surface profile $z(\mathbf{x})$. From Eq. (14),

$$S\varsigma_j\beta_{1j} = \beta_{1j}\frac{\partial}{\partial x_j}z(\mathbf{x}),$$

which gives

$$ST_{0,1}(\mathbf{k}_r,\mathbf{k}_i) = \frac{(1-\rho)(1+\mathrm{R})}{\rho\beta_{rz}+\kappa\beta_{tz}} \times\left\{\frac{1}{(2\pi)^2}\int\int_x \frac{\mathbf{k}_i\cdot\nabla z(\mathbf{x})}{k_1}e^{i(\mathbf{k}_r-\mathbf{k}_i)\cdot\mathbf{x}}d\mathbf{x}\right\}. \tag{29}$$

Inserting the Fourier transform

$$z(\mathbf{x}) = \int\int_{\mathbf{k}_r'-\mathbf{k}_i'} Z(\mathbf{k}_r'-\mathbf{k}_i')e^{-i(\mathbf{k}_r'-\mathbf{k}_i')\cdot\mathbf{x}}d(\mathbf{k}_r'-\mathbf{k}_i')$$

into Eq. (29) yields

$$ST_{0,1}(\mathbf{k}_r,\mathbf{k}_i) = -i\frac{\mathbf{k}_i\cdot(\mathbf{k}_r-\mathbf{k}_i)}{k_1}\frac{(1-\rho)(1+\mathrm{R})}{\rho\beta_{rz}+\kappa\beta_{tz}} \times Z(\mathbf{k}_r-\mathbf{k}_i). \tag{30}$$

For backscatter $\mathbf{k}_r=-\mathbf{k}_i$, $\beta_{rz}=-\beta_{1z}=\sin\theta$, $\mathbf{k}_i^2=\cos^2\theta$, and $\beta_{tz}=[1-(\cos\theta/\kappa)^2]^{1/2}$. When $T_r=hT_{1,0}+ST_{0,1}$ is inserted into Eq. (16), $C(\mathbf{k}_r,-\mathbf{k}_r)$ is obtained for the first order in T. From $C(\mathbf{k}_r,-\mathbf{k}_r)$, the first order perturbation, backscatter cross-section is determined

$$\sigma_p(\theta) = 4k_a^4\sin^4\theta|Y(k_a,\theta)|^2W(2k_a\cos\theta), \tag{31}$$

where

$$Y(k_a,\theta) = \frac{(\rho-1)^2\cos^2\theta+\rho^2-\kappa^2}{[\rho\sin\theta+\sqrt{\kappa^2-\cos^2\theta}]^2} \tag{32}$$

is a modified reflection coefficient that agrees with the result obtained by both Kuo and Moe.[20,21] Substituting the bulk wavenumber and bulk density for a porous soil surface yields the modified reflection coefficient in terms of the surface impedance

$$Y(k_a,\theta) = \frac{[Z-k_a/k_b]^2\cos^2\theta+Z^2-1}{[Z\sin\theta+\sqrt{1-(k_a\cos\theta/k_b)^2}]^2}. \tag{33}$$

The contribution of the impedance to the backscatter strength is then given by

$$S_s(Z,k_b:k_a,\theta) = 20\log|Y(Z,k_b:k_a,\theta)|. \tag{34}$$

Analysis of the ground impedance term given in Eq. (34) shows the sensitivity of acoustic backscatter to impedance effects. The effective flow resistivity spans the broadest range of values for the soil pore properties, from 1000 mks rayls/m for snow to $O(10^6)$ for wet loess surfaces.[22] The contribution of the effective flow resistivity dominates the contribution of the other soil properties for acoustically medium to hard surfaces. Acoustically medium to hard surfaces are defined here as surfaces with an effective flow resistivity of 300 000-mks rayls/m or higher. Typical values range between 1 and 10 for tortuosity and between 0.3 and 0.6 for porosity in soils. The values for tortuosity and porosity will be less than 0.01% of flow resistivity values for acoustically harder surfaces.

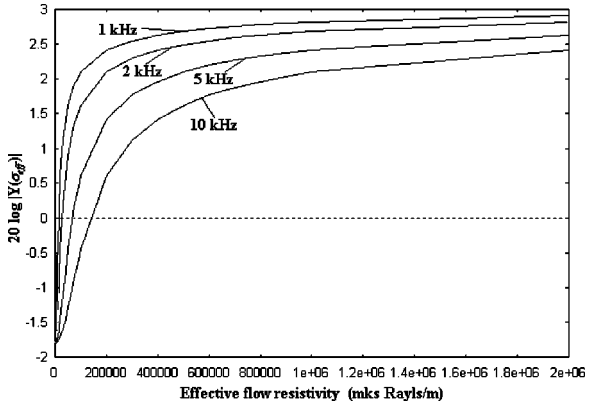

FIG. 5. Contribution of the modified reflection coefficient, $Y(k,\theta)$, versus effective flow resistivity for various frequencies and at a graze angle of 65 degrees.

Figure 5 shows the scatter strength contribution of the modified reflection coefficient for various frequencies versus the effective flow resistivity. The important thing to note is that for frequencies of 10 kHz and below the variation in the contribution of the modified reflection coefficient is less than 1.5 dB for effective flow resistivities of 300 000-mks rayls/m and above. Flow resistivities of 300 000-mks rayls/m and above represent acoustically medium to acoustically hard surfaces. The fact that the contribution of the modified reflection coefficient varies little over these flow resistivity values indicates that the reflection coefficient contribution can be evaluated with minimal error by estimating an appropriate flow resistivity.

The contribution of the modified reflection coefficient is found by choosing likely pore parameters for the surface and evaluating it at a frequency and graze angle. The modified reflection coefficient contribution can then be used to determine the power spectrum of roughness by inverting the backscatter measurement from the perturbation backscatter cross-section. Scatter strength measurements may be inverted to evaluate a point on the power spectrum at some roughness wavenumber

$$S_s(k_a,\theta) = 10\log[4k_a^4\sin^4\theta|Y(k_a,\theta)|^2W(2k_a\cos\theta)], \tag{35}$$

$$10\log W(2k_a\cos\theta) = S_s(k_a,\theta) - 10\log[4k_a^4\sin^4\theta|Y(k_a,\theta)|^2]. \tag{36}$$

If the chosen pore parameters are incorrect, then error will be introduced into the predicted roughness measurement. Since the contribution of the reflection coefficient is dominated by the flow resistivity for acoustically harder surfaces, errors

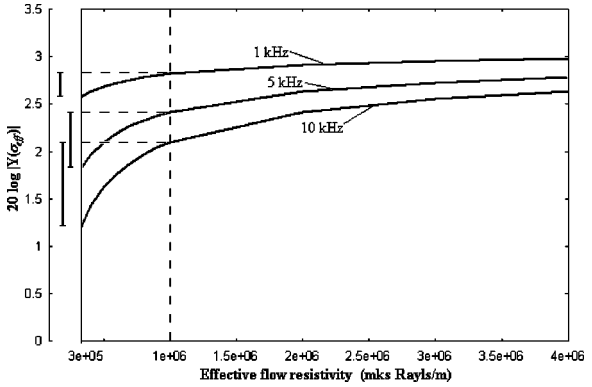

FIG. 6. Range of modified reflection coefficient contribution per range of flow resistivity values for three frequencies.

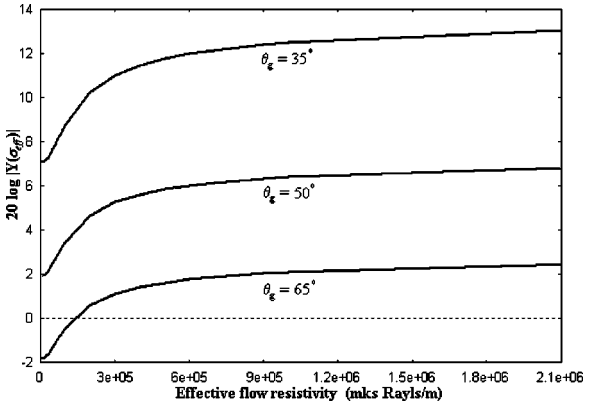

FIG. 7. Contribution of the modified reflection coefficient at various graze angles for 10-kHz signal.

from incorrect choices of tortuosity and porosity have negligible effect. For most outdoor soil surfaces, the frequencies used will be at 10 kHz and below. Assuming an acoustically harder surface and nothing more, the range of choices for the flow resistivity are still very broad. Figure 6 illustrates the range of decibel contribution of the modified reflection coefficient for the range of flow resistivities assumed for an acoustically harder surface. At 5 kHz, choosing an effective flow resistivity of 1×10^6-mks rayls/m, the maximum error introduced into the contribution of the modified reflection coefficient for acoustically medium to hard surfaces is at most about $\frac{1}{2}$ dB. An effective flow resistivity of 1×10^6-mks rayls/m is chosen because it is the middle value within the range of decibel contributions for flow resistivities of 300 000-mks rayls/m and greater. For typical soil surfaces with the rms height calculated for a 60×60-cm^2 section, $\frac{1}{2}$-dB error in the absolute level of the roughness power spectrum translates to about 5.7% error in the rms height calculation. As the frequency is increased, the potential for error from the choice of resistivity of 1×10^6-mks rayls/m increases such that at 10 kHz the maximum error is almost 1 dB to the modified reflection coefficient contribution. At lower frequencies, however, the potential for error from flow resistivity estimations is decreased. At 1 kHz, for example, the error to the modified reflection coefficient is at most about $\frac{1}{4}$ dB for a choice of 1×10^6-mks rayls/m for the flow resistivity. The fact that lower frequencies have less potential for error from the choice of flow resistivity means that mapping out the roughness power spectrum using backscatter may be more accurately accomplished by weighting the measurements taken at lower frequency.

The contribution of the modified reflection coefficient to the overall scatter strength is also affected by the angle of grazing. Figure 7 displays the contribution of the modified reflection coefficient at several graze angles for 10 kHz. The overall effect of the change in graze angle is to raise the absolute level of the reflection coefficient contribution with a slight increase in the slope of the curve for higher flow resistivities. For lower frequencies, the increase in slope of the decibel contribution of the modified reflection coefficient for the higher flow resistivities is even smaller. The impedance effects seen through the contribution of the modified reflection coefficient have a larger effect upon the backscatter strength for smaller graze angles. However, the ability to factor out the impedance effects from the roughness effects rests in the fact that the contribution of the modified reflection coefficient varies little for medium to acoustically hard surfaces. Even for smaller graze angles, errors in choice of flow resistivity yield minimal error in the modified reflection coefficient contribution for medium to acoustically hard surfaces.

It has been shown, theoretically, that the roughness of a porous soil surface can be measured independently from the surface impedance effects for acoustically medium to hard surfaces. The ability to measure the roughness independent from the effects of the pore properties for acoustically medium to hard surfaces using an assumed effective flow resistivity will be examined by experiment. First, backscatter measurements should be taken in the frequency range of 1–10 kHz with different graze angles. A value for the effective flow resistivity, $\sigma_{\text{eff}}=1\times10^6$-mks rayls/m, is assumed in order to calculate the approximate contribution of the modified reflection coefficient to the scatter strength. The roughness power spectrum, evaluated at the roughness wavenumber corresponding to the frequency and graze angle, can be determined by use of Eq. (36) with the modified reflection coefficient and the scatter strength. From the power spectrum, the rms height and correlation length can be calculated. Values for the flow resistivity can be independently measured using a Leonard's apparatus,[23] the method of Stinson and Daigle[24] or a probe microphone technique.[25] From the measured values of the effective flow resistivity, the actual contribution of the modified reflection coefficient can be determined. From the actual value of the modified reflection coefficient the power spectrum, rms height and correlation length can be determined. The effective error in the rms height and correlation length calculation can then be determined by comparing the values obtained with the assumed flow resistivity and the measured flow resistivity.

V. CONCLUSIONS

The scales of roughness for outdoor soil surfaces are typically centimeter in size, which implies that the wavelengths needed to characterize the roughness also be of centimeter size in order to meet the restriction of Eq. (9). Wave-

lengths of this size correspond to frequencies of 10 kHz and below in air. The contribution of the modified reflection coefficient is small and little error is induced by the use of an assumed flow resistivity for frequencies less than 10 kHz. Furthermore, typical weathered soil surfaces have effective flow resistivities of 300 000-mks rayls and greater. For weathered agricultural surfaces an assumed choice of effective flow resistivity, $\sigma_{\text{eff}}=1\times10^{6}$-mks rayls/m, results in minimal error to the value of the modified reflection coefficient. With the maximum possible error of $\frac{1}{2}$ dB to the modified reflection coefficient contribution for a frequency of 5 kHz, the error to the rms height calculation is 5.7%. The error to the rms height is further reduced by taking backscatter measurements at lower frequencies which will have less decibel error to the modified reflection coefficient for the assumed choice of flow resistivity.

Future work will consist of using acoustic backscatter techniques to map out the power spectrums of porous soil surfaces. Presently, the laser profile techniques used to obtain roughness statistics provides more information about a rough surface, however, scan time is extremely long. The acoustic backscatter technique should provide a quick means to obtain the rms height and correlation length statistics for a rough porous surface. The acoustic backscatter technique can then be used in combination with the forward scatter techniques to provide both roughness characterization and pore property characterization for a soil surface.

ACKNOWLEDGMENTS

This research was supported by grants from the USDA through the National Sedimentation Laboratory. We thank Dr. Matt Römkens for his direction in this work.

[1] K. Attenborough, ''Acoustical characteristics of rigid fibrous absorbents and granular media,'' J. Acoust. Soc. Am. **73**, 785–799 (1983).
[2] J. M. Sabatier, H. Hess, W. P. Arnott, K. Attenborough, M. J. M. Romkins, and E. H. Grissinger, ''*In situ* measurements of soil physical properties by acoustical techniques,'' Soil Sci. Soc. Am. J. **54**, 658–672 (1990).
[3] J. M. Sabatier, R. Raspet, and C. K. Fredrickson, ''An improved procedure for the determination of ground parameters using level difference measurements,'' J. Acoust. Soc. Am. **94**, 396–399 (1993).
[4] K. Attenborough, S. I. Hayek, and J. M. Lawther, ''Propagation of sound above a porous half-space,'' J. Acoust. Soc. Am. **68**, 1493–1501 (1980).
[5] K. Attenborough, ''Review of ground effects on outdoor sound propagation from continuous broadband sources,'' Appl. Acoust. **24**, 289–319 (1988).
[6] K. Attenborough and S. Taherzadeh, ''Propagation from a point source over a rough finite impedance boundary,'' J. Acoust. Soc. Am. **98**, 1717–1722 (1995).
[7] M. S. Howe, ''On the long range propagation of sound over irregular terrain,'' J. Sound Vib. **77**, 83–94 (1985).
[8] I. Tolstoy, ''Coherent sound scatter from a rough interface between arbitrary fluids with particular reference to roughness element shapes and corrugated surfaces,'' J. Acoust. Soc. Am. **72**, 960–972 (1982).
[9] J. P. Chambers, R. Raspet, and J. Sabatier, ''Incorporating the effects of roughness in outdoor sound propagation models,'' in *Proceeding of Noise-Con '96* (Conference on Noise Control Engineering, Seattle), pp. 905–910 (1996).
[10] M. J. M. Römkens, J. Y. Wang, and R. W. Darden, ''A Laser Microreliefmeter,'' Trans. *ASAE* **31**(2), 408–413 (1988).
[11] M. J. M. Römkens and J. Y. Wang, ''Roughness and sealing effect on soil loss and infiltration on a low slope,'' Advances in GeoEcology **31**, 589–595 (1998).
[12] A. N. Kolmogorov, ''On the logarithmic normal distribution rules of dimensions of particles by grinding,'' Mathematika **31**, 99–101 (1971).
[13] D. R. Jackson, D. P. Winebrenner, and A. Ishimaru, ''Application of the composite roughness model to high-frequency bottom backscattering,'' J. Acoust. Soc. Am. **79**, 1410–1422 (1986).
[14] R. J. Urick, *Principals of Underwater Sound* (McGraw-Hill, New York, 1983).
[15] J A Ogilvy, *Theory of Wave Scattering from Random Rough Surfaces* (Adam Hilger, Bristol, England, 1991).
[16] D. R. Jackson, K. B. Briggs, K. L. Williams, and M. D. Richardson, ''Tests of models for high-frequency seafloor backscatter,'' IEEE J. Ocean Eng. **21**, 458–470 (1996).
[17] D. R. Jackson and K. B. Briggs, ''High frequency bottom backscattering: Roughness versus sediment volume scattering,'' J. Acoust. Soc. Am. **92**, 962–977 (1992).
[18] P. D. Mourad and D. R. Jackson, ''High frequency sonar equation models for bottom backscatter and forward loss,'' in *Proceedings of Oceans '89* (Marine Technology Society and IEEE Oceanic Engineering Society, Seattle, 1989), pp. 1168–1989.
[19] E. I. Thorsos and D. R. Jackson, ''The validity of the perturbation approximation for rough surface scattering using a Gaussian roughness spectrum,'' J. Acoust. Soc. Am. **86**, 261–277 (1989).
[20] E. Y. T. Kuo, ''Wave scattering and transmission at irregular surfaces,'' J. Acoust. Soc. Am. **36**, 2135–2142 (1964).
[21] J. E. Moe and D. R. Jackson, ''First-order perturbation solution for rough surface scattering cross section including the effects of gradient,'' J. Acoust. Soc. Am. **96**, 1748–1754 (1994).
[22] K. Attenborough, ''Ground parameter information for propagation modeling,'' J. Acoust. Soc. Am. **92**, 418–427 (1992).
[23] R. W. Leonard, ''Simplified flow resistance measurements,'' J. Acoust. Soc. Am. **17**, 240–241 (1946).
[24] M. R. Stinson and G. A. Daigle, ''Electronic system for the measurement of flow resistance,'' J. Acoust. Soc. Am. **83**, 2422–2428 (1988).
[25] J. M. Sabatier, D. C. Sokol, C. K. Fredrickson, M. J. M. Römkens, E. H. Grissinger, and J. C. Shipps, ''Probe microphone instrumentation for determining soil physical properties: testing in model porous materials,'' Soil Tech. **8**, 259–274 (1996).